

EFFICIENCY OF CONTEXTUAL INFORMATION IN PROCESSING OF INTERFEROMETRIC DATA STACKS

Roghayeh Zamani¹, Hossein Aghababaei², and Giampaolo Ferraioli³

^{1,3} University of Napoli, Parthenope, Napoli, Italy.

² University of Twente, Enschede, the Netherlands.

ABSTRACT

Among available methods for geodetic measurements, synthetic aperture radar (SAR) interferometry (InSAR) has been considered as a powerful tool for the monitoring of earth's surface, digital elevation model generation and possible slow temporal deformation mapping. In this context, multi-baseline SAR interferometry with the availability of multiple interferograms obtained from multi-pass satellite observations significantly improves the accuracy of the estimated target's parameters, *i.e.* the residual height and the mean deformation velocity. In this paper contextual spatial information has been exploited as a regularization term in order to improve the capability of multibaseline SAR Interferometry in dealing with possible artifacts and outliers induced by temporal decorrelation and remained atmospheric phase noise effects which can impair the accuracy of estimated target's parameters. The superiority of regularized processing is related to depletion of velocity variations over the scene and reducing ambiguity in parameter estimation. The proposed method is evaluated using a simulated and a real data set acquired by COSMO-SkyMed sensor over Tehran, Iran; and the results are compared with conventional adapted approach in the literature. The evaluation indicated that adaptation of contextual information can significantly improve the interferometric-based parameter estimation over partially coherent targets which are affected by outliers and artifacts.

Index Terms— Synthetic aperture radar (SAR), Multi-baseline SAR interferometry, Regularization term, Contextual information.

1. INTRODUCTION

The differential synthetic aperture radar (SAR) interferometry is today well assessed and broadly exploited in order to accurately measure the Earth's surface displacements [1, 2]. The conventional interferometric technique employs two SAR images acquired from slightly different angles, in which the information of elevation and deformation can be captured through the processing of the phase difference or the so-called interferometric phase [3]. In this context, a wealth of information in deformation

mapping and digital elevation model (DEM) generation can be obtained through the use of multi-temporal time series SAR data [1-4].

Persistent scatterer interferometry (PS InSAR) [2] and coherent stacking interferometry (CS InSAR) [1] are the main multi-baseline interferometric techniques that have been frequently employed in the literature. PS InSAR has been recognized as one of the first and typical techniques for the interferometric analysis that operates at the full spatial resolution. Instead, CS InSAR generally uses multi-looking operation in order to increase the interferometric phase quality. Within the framework of multi-look MB interferometry, a methodology that brought the analysis of data covariance matrix to the interferometric technique was reported by the so-called SqueeSAR technique [1]. The method is an extension of the PS-InSAR approach and estimates the covariance matrix using a spatial multi-looking operation in order to spread the PS-InSAR processing to both deterministic and distributed (or partially coherent) targets. The phase triangulation of the covariance matrix is proceeded and consequently, the optimized values of the interferometric phase are obtained for PS-InSAR analysis. Although, SqueeSAR may mitigate the noise effects by improving the interferometric phase quality of the partially coherent. however, the technique relies only on the use of phase information rather than taking the benefits of full information of the data covariance matrix. The other multi-baseline interferometric technique using the data covariance matrix is the Maximum-likelihood (ML) estimation procedure. Unlike SqueeSAR, ML employs full information of the data covariance matrix.

Typically, these techniques require the scatterer to possess some fundamental specifications: the target's reflectivity is constant over all acquisitions and its interferometric phase is related to the nominal distance between sensor and target. In reality, however, temporal decorrelation and un-modeled phase error (e.g. from non-optimal atmospheric compensation) can significantly compromise the performance of these techniques.

In this paper, in order to cope with the above-mentioned issues and mitigate their destructive effects the proposed approach adds a regularization term (or a constraint) to the ML's model in order to include the information about the scene velocity variation. Hence, the resulted non-convex

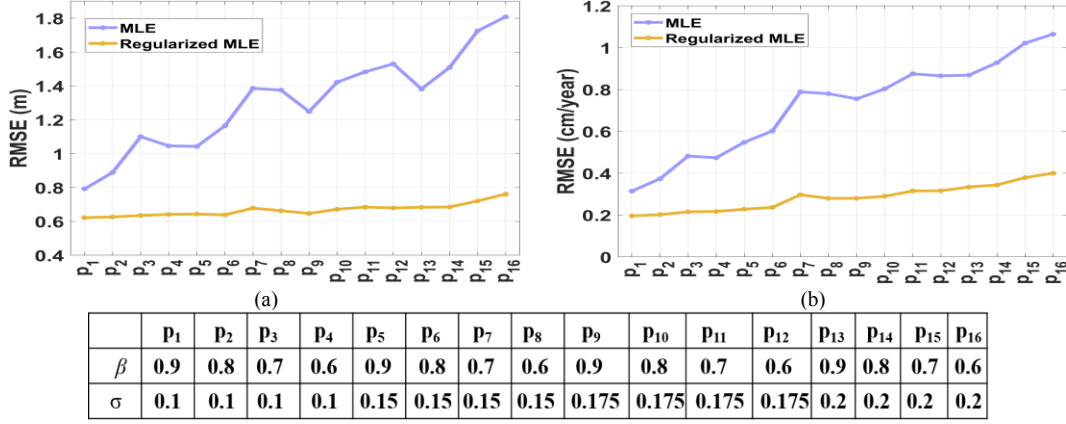


Fig. 1. Evaluation of the employed approaches with respect to different temporal decorrelation β and atmospheric σ effects.

with respect to a given master image, and accuracy compensated to the atmospheric phase error. Therefore, the resulting complex target vector \mathbf{x} for a specific pixel p can be represented by [1]:

$$\mathbf{x}(p) = [x_1(p) \ x_2(p) \ \cdots \ x_N(p)]^T \quad (1)$$

where T indicate the transpose operator. The measured multi-baseline target vector $\mathbf{x}(p)$ has circular Gaussian random distribution with zero mean and its covariance matrix is given by $\mathbf{R} = E\{\mathbf{x}(p)\mathbf{x}(p)^H\}$, where E and H are the expectation and Hermitian operators, respectively.

The distribution of \mathbf{x} is represented as [5]:

$$f(\mathbf{x} | \mathbf{R}) = \exp\left(-\mathbf{x}^H \mathbf{R}^{-1} \mathbf{x}\right) / \pi^N |\mathbf{R}| \quad (2)$$

Note that in (2), the dependence of \mathbf{x} and \mathbf{R} on the pixel coordinates p has not explicitly indicated for the sake of notation simplicity. The data covariance matrix \mathbf{R} can be transformed into the coherence matrix \mathbf{C} through the following equation.

$$\mathbf{R} = \mathbf{\Gamma}^{1/2} \mathbf{C} \mathbf{\Gamma}^{1/2} \quad (3)$$

Where $\mathbf{\Gamma}$ is a diagonal matrix constructed by the diagonal elements of \mathbf{R} , in which $\mathbf{\Gamma}(k,k)$ represent the reflectivity of k^{th} image channel, while \mathbf{C} is coherence matrix where its elements can be given by the following equation [1].

$$\mathbf{C}(k,l) = \gamma_{kl} \exp(i\varphi_{kl})$$

$$\varphi_{kl} = (4\pi B_{kl} / \lambda \rho \sin(\theta)) z + (4\pi T_{kl} / \lambda) v = k_z z + \xi_{kl} v \quad (4)$$

where, γ_{kl} and φ_{kl} are the real valued coherence and interferometric phase between channels k and l , respectively. Moreover, the parameters B , T , λ , ρ , and θ indicate the spatial orthogonal baseline, temporal baseline, system wavelength, sensor to target range distance and look angle, respectively. In (4), z and v represent the residual height and mean velocity. It has to be understood that the data are assumed to be compensated to the flat-earth and topographic phase effects, *i.e.* using low resolution external terrain model such as SRTM, and atmospheric effect has been removed while the noise contribution is omitted.

It can be easily shown that the maximum likelihood

estimation from nonlocal approach *i.e.* $\gamma_{kl} = \hat{\gamma}_{kl}^{\text{NL}}$ where $\hat{\gamma}_{kl}^{\text{NL}}$ is a real value coherence between channels k and l obtained from the non-local coherence matrix $\hat{\mathbf{C}}^{\text{NL}}$.

2.1 Contextual-based Interferometry

In this paper, to enhance the estimation accuracy, the use of contextual information is investigated. Following the idea proposed in [7, 8], we proposed to combine the solution of typical MLE optimization in (5) and the velocity variation in the neighborhood pixels. The proposed framework is based on the fact that the mean velocity is nearly constant from pixel to pixel and it smoothly change over the study areas. Hence, a priori that can control the velocity variation between neighborhood pixels is given by $\Sigma_q |v(p) - v(q)|$, where $v(p)$ and $v(q)$ are the mean velocities of pixels p and q . This term as a contextual information represents the total variation of velocity within the neighbourhood of pixel p . In this papers, this term is added to the ML based optimization algorithm. Hence, Eq. (5) can be refined as:

$$(\hat{z}, \hat{v}) = \arg \min_{z, v} \sum_{p,q} \left[\text{Trace}(\mathbf{C}^{-1} \hat{\mathbf{C}}^{\text{NL}})_{p,q} + \alpha |v(q) - v(p)| \right] \quad (6)$$

Equation (6) indicates the maximum likelihood estimation regularized with the defined contextual information. In particular, the residual height and mean velocity should be estimated in such a way that the function $\text{trace}(\mathbf{C}^{-1} \hat{\mathbf{C}}^{\text{NL}})$ which called data term, is minimized under the constraint that the difference of the velocity of pixel p with respect to its neighborhoods is a minimal value. In the above equation, α is a balancing parameter controls the relative importance of the two terms. Unlike to Eq. (5), the optimization of (6) turn to be difficult. To this aim a graph cut minimization based strategy [9] is adapted. From the selected pixel and its neighborhood, a graph at L elevation-velocity layers is built, where the nodes of the graph are related to the data terms, *i.e.* $\text{trace}(\mathbf{C}^{-1} \hat{\mathbf{C}}^{\text{NL}})$. Then the solution of (6) can be obtained by seeking for a graph-cut whose sum of data term and velocity variation in all pixels along the graph-cut is the minimum between all other possible cuts. As a final remark, it should be noted that the

parameter α is tuned by trial and error in our implementation.

3. EXPERIMENTAL RESULTS

3.1. Simulated data

The Monte Carlo simulations were proceeded in order to simulated a stack of 19 images (with a size of 512×512), where the spatial and temporal baselines as well as the system parameters, are set to the typical values of the COSMO-SkyMed data set. The data were simulated in a favorable scenario over particular terrain height model and the true imposed velocity map. In order to evaluate the efficiency of the proposed method, simulated data are corrupted with some artifacts i.e. temporal decorrelation and atmospheric noise effects in 50% of pixels of the simulated image. To impair the data by temporal decorrelation, the coherences are affected by the well-known decorrelation model as $\gamma_{kl} = \gamma_{kl} \exp(-|t_l - t_k|/\tau)$, where τ is the decorrelation rate, while the atmospheric phase noise is simulated with zero mean and standard deviation of $\sigma\pi$ from baseline to baseline. The decorrelation rate is set to the particular $\beta\%$ of the total temporal baseline (T), i.e. $\tau = \beta T$. To the aim of extensive analyses, the corruptions were proceeded by variation of both parameters in the range of $\beta \in [0.9 \ 0.8 \ 0.7 \ 0.6]$ and $\sigma \in [0.1 \ 0.15 \ 0.175 \ 0.2]$. For each pair of (β, σ) , both conventional and regularized MLs were implemented. For each pair of (β, σ) , the root mean square error (RMSE) between the estimated and true values of the elevation and velocity maps are computed and plotted in Fig. 1. The RMSE for both elevation and velocity affirms the performance of the proposed method compared with the conventional ML approach.

4. CONCLUSION

In this paper, a new framework for the estimation of target parameters (residual height and deformation mean velocity) using MB interferometric data sets was introduced. The proposed method adapts a regularization of the velocity variation over neighborhood pixels into the ML model. The quantitative and qualitative analyses were carried out to validate the effectiveness of the proposed method. It is shown that the proposed procedure is robust to the outliers and artifacts. Particularly, the method employs the information of neighborhood pixels to provide a reliable solution for the pixel of interest (central pixel), which is impaired by disturbing factors. Note that the improvement by the regularization is paid at the cost of computational efforts.

REFERENCES

[1] P. Berardino, G. Fornaro, R. Lanari, and E. Sansosti, "A new algorithm for surface deformation monitoring based on small baseline differential

SAR interferograms," *IEEE Transactions on Geoscience and Remote Sensing*, vol. 40, no. 11, pp. 2375-2383, 2002.

[2] A. Ferretti, C. Prati, and F. Rocca, "Nonlinear subsidence rate estimation using permanent scatterers in differential SAR interferometry," *IEEE Transactions on Geoscience and Remote Sensing*, vol. 38, no. 5, pp. 2202-2212, 2000.

[3] R. Bamler and P. Hartl, "Synthetic aperture radar interferometry," *Inverse problems*, vol. 14, no. 4, p. R1, 1998.

[4] A. Ferretti, A. Fumagalli, F. Novali, C. Prati, F. Rocca, and A. Rucci, "A New Algorithm for Processing Interferometric Data-Stacks: SqueeSAR," *IEEE Transactions on Geoscience and Remote Sensing*, vol. 49, no. 9, pp. 3460-3470, 2011.

[5] J. W. Goodman, "Some fundamental properties of speckle," *JOSA*, vol. 66, no. 11, pp. 1145-1150, 1976.

[6] C.-A. Deledalle, L. Denis, F. Tupin, A. Reigber, and M. Jäger, "NL-SAR: A unified nonlocal framework for resolution-preserving (Pol)(In) SAR denoising," *IEEE Transactions on Geoscience and Remote Sensing*, vol. 53, no. 4, pp. 2021-2038, 2015.

[7] G. Ferraioli, C. A. Deledalle, L. Denis, and F. Tupin, "Parisar: Patch-Based Estimation and Regularized Inversion for Multibaseline SAR Interferometry," *IEEE Transactions on Geoscience and Remote Sensing*, vol. 56, no. 3, pp. 1626-1636, 2018.

[8] H. Aghababae, G. Ferraioli, G. Schirinzi, and V. Pascazio, "Regularization of SAR Tomography for 3-D Height Reconstruction in Urban Areas," *IEEE Journal of Selected Topics in Applied Earth Observations and Remote Sensing*, vol. 12, no. 2, pp. 648-659, 2019.

[9] H. Ishikawa, "Exact optimization for Markov random fields with convex priors," *IEEE Transactions on Pattern Analysis and Machine Intelligence*, vol. 25, no. 10, pp. 1333-1336, 2003.